sciendo
DOI: 10.1515/agriceng-2019-0023

ISSN 2083-1587; e-ISSN 2449-5999
2019, Vol. 23, No.3, pp. 29-39
Agricultural Engineering
www.wir.ptir.org

STRESS ANALYSIS OF THE SUGAR BEET LIFTER WITH THE FINITE ELEMENT METHOD (FEM)

Marek Boryga [a], Paweł Kołodziej[b*]

[a] Department of Mechanical Engineering and Automation, University of Life Sciences in Lublin, Poland, ORCID 0000-0002-5991-7871
[b] Department of Mechanical Engineering and Automation, University of Life Sciences in Lublin, Poland, ORCID 0000-0003-0479-1770

** Corresponding author: e-mail: pawel.kolodziej@up.lublin.pl*

ARTICLE INFO

Article history:
Received: August 2019
Received in the revised form: August 2019
Accepted: September 2019

Keywords:
passive sugar beet lifter,
stress analysis
finite element method (FEM)
system with adjustable torsional stiffness

ABSTRACT

The article presents the method of creating a 3D model of a passive lifter with (polder) plowshares, used in sugar beet harvesters, along with stages of its preparation and results of stress analysis. The computer simulation takes into account force timelines obtained during field tests of the tool. The *Stress analysis* module of the *Autodesk Inventor* program was used for the analysis, using the finite element method (FEM). The analysis included the elements that constitute the working part of the lifter, whereas elements of the flexible system were omitted. The results confirm that the lifter structure was developed correctly in terms of durability. The highest reduced stresses, calculated according to the Huber-Mises-Hencky (HMH) hypothesis, were 128.4 MPa (the minimum value of the safety factor related to the yield point is 1.61). The paper also discusses the construction of two flexible couplings with infinitely variable torsional stiffness, which can be used as an alternative solution for a typical flexible system: a shock absorber and a helical spring.

Introduction

The ongoing development of design systems, and the growing requirements of the modern engineering industry prompt designers to use the latest computer-aided design methods and tools. Modern design systems allow not only to build a 3D model, but also to carry out many virtual prototype tests (stress and strain analyses, modal analyses, parameterization, optimization tests, etc.). Virtual prototyping reduces the costs of construction and testing of real objects and the deployment itself. Moreover, it enables a multi-variated analysis of a structural solution and can be used both for the entire structure and for a single subassembly or element (Pawłowski and Szczepaniak, 2005; Dębski et al., 2012; Korzybski and Rode, 2014; Łukasiewicz, 2017).

The use of design support systems in scientific research was of interest to many researchers. Some of the published works relate to the design or verification of elements and devices used in agriculture. Celik et al. (2009) carried out a FEM analysis of a plumbing element used in field irrigation. They built a 3D model of the element, assessed the operating conditions, and then conducted tests to determine the optimal thickness and length of the body using the results of stress analysis. Patyk and Kukiełka (2009) conducted modeling and simulation of the phenomenon of the fatigue wear of a cultivator tooth. In the modeling process, they used an incremental, updated Lagrangian description and adequate measurements of stress and strain increases. The computer simulations were conducted using the ANSYS/Ls-Dyna system. On the other hand, Malon et al. (2016) designed and optimized the chassis of the air assisted sprayer. Based on an agricultural machine with similar characteristics, they created an original 3D model, and then performed stress and displacement analyses using FEM on six cases of device-specific operating workloads. The authors stated that the test results and subsequent optimization allowed to reduce the mass of the chassis by 18.5%, as compared to the original model. Additionally, Choi et al. (2018) analyzed a multi-stage cylindrical gear used in an electric agricultural vehicle. In order to increase the gear's service life, they conducted modal and stress analyses using FEM (the ANSYS system). The aim of the work was achieved by creating an appropriate tooth surface profile.

High efficiency and a wide area of application of computer-aided design methods allows creating 3D models of various elements and components of agricultural machinery. This also applies to lifter units of sugar beet harvesters. Currently used lifters are most often equipped with vibrating mechanisms. In addition to the main function, i.e. releasing roots from the growth area, the tool is also used to break the soil, in order to reduce energy expenditure associated with the beet harvest (Dykstra, 1996; Herrmann, 1996). As a rule, the construction of lifters includes active units, equipped with swinging beams with disc (polder) plows, which are driven by (eccentric) cam shafts and hydraulic motors. The amplitude of the forced vibrations is constant during the lifter's operation, and their frequency can be adjusted by changing the rotational speed of the eccentric. Active units are most often multi-row mechanisms and, due to the extensive drive and movement control systems of individual actuators, are technically advanced. However, these are devices that generate significant costs, e.g. energy consumption, servicing, purchase, etc.

Another type of lifters is vibrating passive units, the design of which includes pivotally mounted beams with plowshares, connected to the frame via a spring element (Boryga and Kołodziej, 2019). The mechanism is excited by the vibrations that arise as a result of movement resistance during operation of the harvester. Tests of the passive device with a spiral spring element demonstrate that an appropriate adaptation of its flexibility allows a resonance frequency that loses the soil and saves energy (Švrcek, 1995). Therefore, it is appropriate to look for construction solutions that allow the flexible system to be inserted into the passive lifter mechanism, to change its rigidity during operation.

The purpose of the paper is to design the mechanical system of the sugar beet harvester passive lifter, and analyze of the strain of its structural elements, taking into account the timelines of forces obtained on the basis of field tests (Kołodziej and Gołacki, 2006). The analysis was carried out using the *Stress analysis* module of the program *Autodesk Inventor*. The results were presented in the form of reduced stress distribution maps calculated according to the Huber-Mises-Hencky (HMH) hypothesis. In addition, it was proposed to equip the passive lifter with mechanisms enabling the change of the structure's own vibration frequency, depending on operating conditions.

Material and methods

Fig. 1 shows a 3D model of a passive sugar beet lifter. The body of the lifter consists of a welded supporting structure, comprising a rotary sleeve 1, swinging frame plate 2, lifter columns 3, lifter columns tips 4 and plate 5. The lifter is further equipped with profiled inserts 6, shares 7, angle struts 8, guide rod holders 9, guide rods 10, and the flexible system 11, comprising a spring, shock absorber and fixing elements.

The solid model of the first element, which was rotary sleeve 1, was created using a template *Standard.ipt*. Other elements: the swinging frame plate 2, lifter columns 3, lifter columns tips 4 and plate 5 were created in the template *Weldment.iam* and connected using the tool *Welds*.

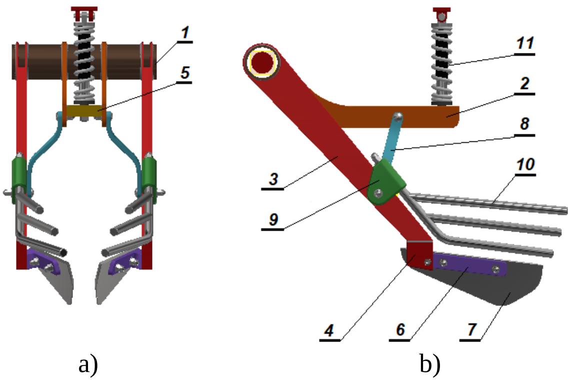

Figure 1. 3D model of a passive sugar beet lifter (1 − rotary sleeve, 2 − swinging frame plate, 3 – lifter columns, 4 – lifter columns tips, 5 – plate, 6 – profiled inserts, 7 – shares, 8 – angle struts, 9 – guide rod holders, 10 – guide rods, 11 – flexible system): a) main view, b) left view, c) top view

Fig. 2 demonstrates the welded joints of the rotary sleeve with the swinging frame plate and the lifter columns, the lifter column with the tip, the swinging frame plate with the plate, and the lifter column with the sleeve.

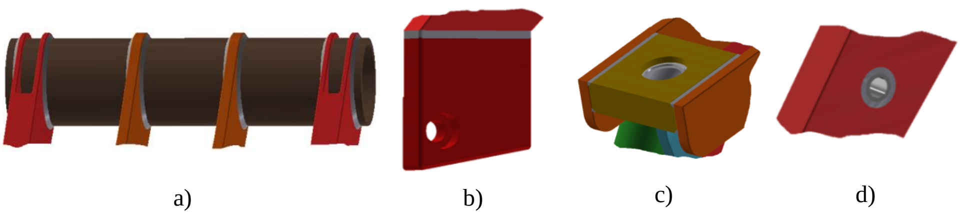

Figure 2. Welded connections of the lifter: a) rotary sleeve with swinging frame plate and lifter columns, b) lifter column with the tip, c) swinging frame plate with plate, d) lifter column with sleeve

In addition, solid models of profiled inserts 6, shares 7, angle struts 8, guide rod holders 9, guide rods 10 and of flexible system components 11 were created. Fig. 3 presents details of the connection of the listed elements. The profiled inserts are elements that allow to precisely position the shares in space. The shares are attached to the inserts with plow bolts, washers and cap nuts, while the profiled inserts are attached to the tips of the lifter columns with single bolts, using a form-fitting connection (Fig. 3a). The guide rod holders are attached to the lifter columns using single mushroom and square bolts, washers and cap nuts. The same bolts are used to connect the angle struts to the lifter columns. To connect the guide rods inside the handles, a polygonal connection was used, secured against axial displacement by a bolted connection (Fig. 3b). A clevis fastener and a bolted connection were used to connect the shock absorber (Fig. 3c).

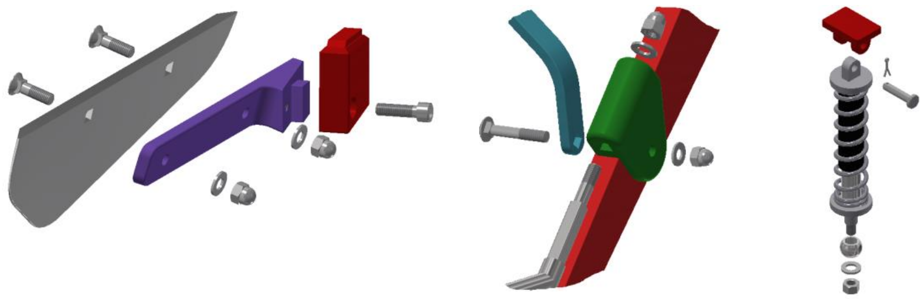

a) b) c)

Figure 3. Disconnectable connections: a) share with profiled insert and lifter column tip, b) lifter column, rod holder, guide rods and angle strut, c) shock absorber with spring, base and bearing

Static analysis procedure in the module *Stress analysis* of the program *Autodesk Inventor* included the following stages (Fig. 4). At the initial stage, a simplification was made by excluding the elastic-damping system comprising a shock absorber, helical spring and standard elements, i.e. bolts, nuts and washers from the scope of simulation analysis. Then, the materials of individual elements were defined, but only those defined in *Autodesk Inventor*'s database were used.

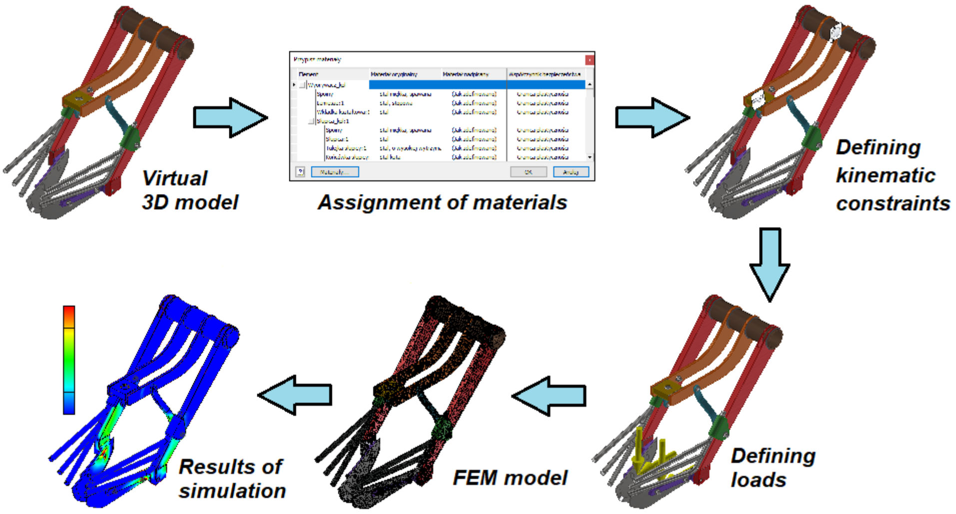

Figure 4. Stages of FEM simulation

The choice of materials for lifter elements was preceded by an analysis of their mechanical properties. The properties of the materials used are summarized in Table 1.

Table 1.
Mechanical properties of the materials used

Material	ν (-)	E (GPa)	R_e (MPa)	R_m (MPa)	ρ (g·cm^{-3})	Elements
Steel	0.3	210	207	345	7.85	Lifter column, profiled insert, swinging frame plate, spring plate, guide rod holder, guide rods, angle strut
Forged steel	0.3	210	250	300	7.85	Lifter column tip
Alloy steel	0.3	205	250	400	7.73	Shares, bearing housing
High strength steel, low alloy	0.29	200	275.8	448	7.85	Sleeve
Mild steel, welded	0.28	220	207	345	7.85	Welds

Material	ν (-)	E (GPa)	R_e (MPa)	R_m (MPa)	ρ ($g \cdot cm^{-3}$)	Elements
Mild steel	0.28	220	207	345	7.85	Standard elements

In the next stage, kinematic constraints and forces acting on lifter shares were introduced. When introducing the constraints, fixed bonding (on the surface of the bearing body) and pin bonding (on the internal surface of the lifter's sleeve) were used.

The external load acting on the lifter shares was determined based on the results of field tests. Fig. 5 shows examples of timelines of the horizontal and vertical components of the force acting on the tool (Kołodziej and Gołacki, 2006).

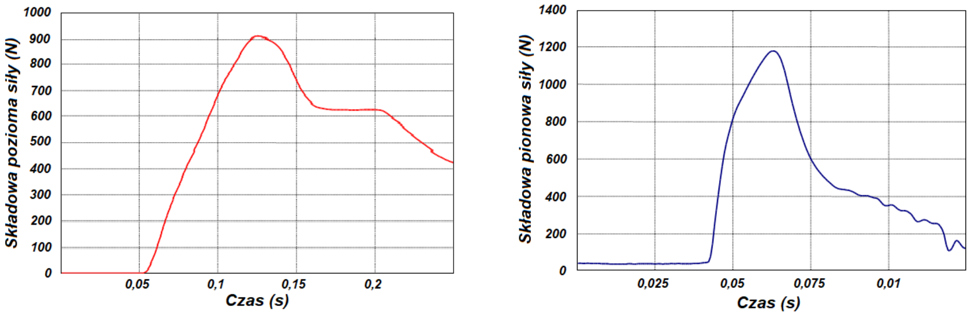

a) b)

Figure 5. The course of the force components acting on the lifter blade a) horizontal component, b) vertical component

Bonds contact were generated in the 3D model, which were used for all analyzed elements of the lifter. No changes have been made to the mesh settings, as compared to the standard settings (*average element size* – 0.1, *minimum element size* – 0.2, *grading factor* - 0.5, *maximum turn angle* – 60°), but it was decided that the convergence settings be changed *maximum number of h refinements* – 8, and the *stop criteria* was 5%. These settings mean that the program would perform calculations several times (maximum 8), each time modifying the mesh in places of maximum stress, until the difference in results in subsequent repetitions is less than 5%. The last stage was to run the simulation and analyze the results.

Results and discussion

Fig. 6 shows the distribution of reduced stress of the lifter, calculated according to the HMH hypothesis. The number of mesh elements was 318461, and the number of nodes 562498. In order to enable a more accurate observation of the differences in the concentration of the reduced stresses in various elements of the lifter unit, the maximum threshold value was changed to 15 MPa.

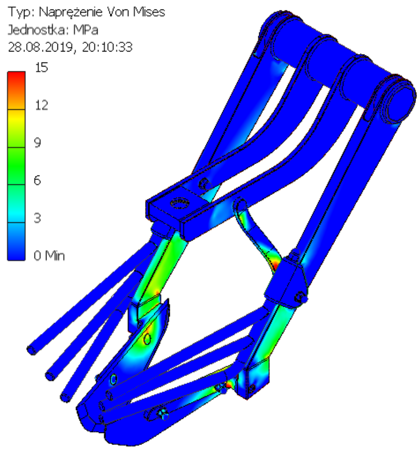

Figure 6. Distribution of reduced stresses in the 3D model of the lifter

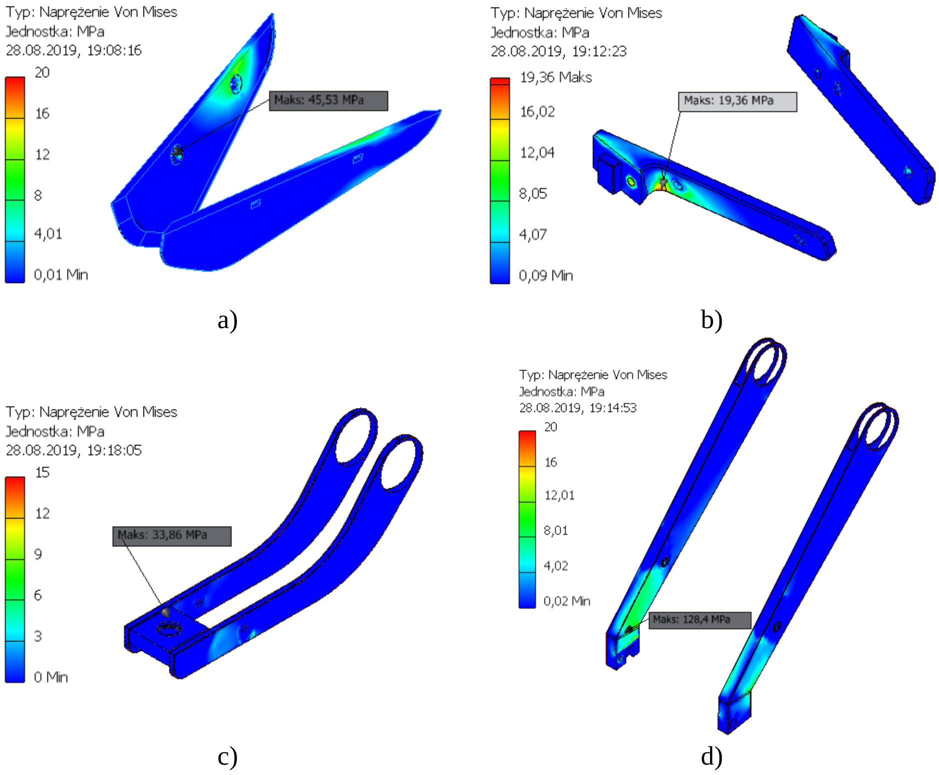

Figure 7. Distribution of reduced stresses in individual elements of the lifter's 3D model: a) shares, b) profiled inserts, c) swinging frame plate, d) lifter columns with tips

Fig. 7 demonstrates the reduced stress distributions for the four elements of the lifter, in which the highest reduced stress values were observed, i.e. in shares, profiled inserts, the swinging frame plate and angle struts. As in the case of Fig. 6, in order to enable a more accurate observation of the differences in the concentration of reduced stresses, the maximum threshold value was adjusted.

Maximum values of reduced stress, 128.4 MPa, occurred at the connections between the lifter columns and tips. In the case of shares, the largest stress value of 45.53 MPa was recorded in the sockets for the heads of the bolts securing the share to the profiled insert. The highest stress concentration (maximum value: 33.86 MPa) for the swinging frame plate occurred at the place of attachment of the flexible system. In the case of the profiled insert, the maximum reduced stress of 19.36 MPa occurred at the point of profile change.

The determined stress values can be used for preliminary assessment of the mechanical strength of the working part of the lifter, and to make future changes and constructional modifications of the machine. Fig. 8 presents two constructional solutions of mechanisms attached to the lifter columns, which enable control of the system's flexibility. The proposed solutions would fulfill the role of a typical flexible system, comprising a shock absorber and helical spring, and at the same time enabling the adjustment of the stiffness to the working conditions of the lifter.

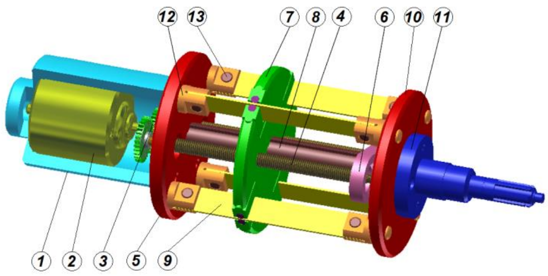

a)

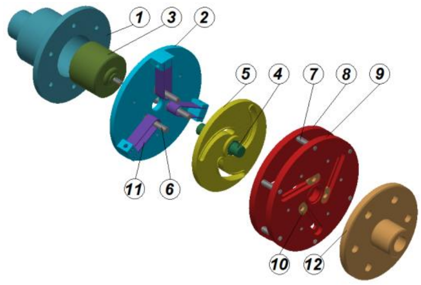

b)

Figure 8. Flexible system with adjustable torsional stiffness a) with axial springs, b) with radial springs

In the first structural solution (Kołodziej and Stępniewski, 2007; Kołodziej and Boryga, 2014; Kołodziej and Boryga, 2017), flat springs were used, parallel to the axis (Fig. 8a). The hollow input shaft 1 has a built-in stepper motor 2, driving a lead screw 4 through a gearing 3. The rotable screw in the active plate 5 and thrust plate 6 is used to move the control disk 7. The axial displacement of the control plate along the spline shaft 8 causes a change in the active length of the flat springs 9, while changing the torsion angle between the active plate

5 and the passive plate 10, to which the output shaft 11 is connected. The flat springs are rigidly fixed with pins 13 in holders 12, which can rotate freely in the discs 5 and 10. The maximum compliance of the system was obtained in a position where the control disk 7 is closest to the active disk 5, while the minimum – when the control disk was closest to the thrust disk 6.

In the second construction solution (Pater et al., 2017; Boryga and Kołodziej, 2018), U-shaped springs were used, located radially (Fig. 8b). The system was constructed of a hollow input shaft 1, combined with active disk 2. Inside the shaft, a stepper motor 3 is built-in, driving a control plate 5 through the splined shaft 4. The control plate has three spiral guide channels, the surfaces of which cooperate with three pins of the springs 6. The control disk 5 was placed between two thrust disks, internal 8 and external 9, (connected by pins 7). Oblique guide channels were made in thrust disks. The channels have sliders 10, to fix the position of the spring pins 6. Pins 6 cooperate with both sliders 10, and springs 11, the ends of which are fixed in the grips of the active plate 2. External thrust plate 8 was connected to the output element in the form of a plate 12. Adjustment of compliance was achieved by changing the active length of the springs 11, as a result of radial displacement of the spring pins 6 during the rotation of the control plate 5. The maximum compliance of the system was obtained for the position, in which the spring pins 6 were closest to the free ends of the springs 11, while the minimum - when the pins 6 were closest to the spring restraint 11.

Conclusions

Based on the presented analysis, it can be stated that:

1. The greatest reduced stress of the working part of the lifter, calculated on the basis of the HMH hypothesis of 128.4 MPa, occurred at the connections of the lifter columns and tips. The calculated value of the safety factor related to the yield point was 1.61. In other structural elements, the coefficient value was much higher.
2. Used in FEM analysis, the force courses obtained from bench tests allows to determine as realistic stress distributions as possible.
3. Solid modeling, combined with stress analysis, streamlines the design process and allows structural adjustments and modifications before creating the prototype.
4. Connected with the rotary sleeve, the presented two constructional solutions of devices with adjustable compliance can effectively change the frequency of the working sequence of the mechanism. The selection of the type of the flexible system depends on the geometrical parameters of the lifter unit.

References

Boryga, M., Kołodziej, P. (2018). Numerical verification of the correctness of the modelling clutch with adjustable torsional. *Mechanik, 10*, 838-841.

Boryga, M., Kołodziej, P. (2019). Dynamic analysis of sugar beet lifter. *Journal of Research and Applications in Agricultural Engineering, 64*(2), 19-24.

Celik, H.K.,Topakci, M., Akinci, I. (2009). Structural optimization with FEM in agricultural engineering: a case study for irrigation plumbing element. *Proceedings 37th International Symposium „Actual tasks on agricultural engineering"*, Opatija, Croatia, 497-506.

Choi, W.S., Pratama, P.S., Supeno, D., Jeong, S.W., Byun, J.Y., Woo, J.H., Lee, E.S., Park, C.S. (2018). Characteristics of reduction gear in electric agricultural vehicle. *5th International Conference on Mechanical Engineering, Materials Science and Civil Engineering 324*, Article Number: 012036.

Debski, H., Koszalka, G., Ferdynus, M. (2012). Application of fem in the analysis of the structure of a trailer supporting frame with variable operation parameters. *Eksploatacja i Niezawodność – Maintenance and Reliability, 14*(2), 107-113.

Dykstra, M. (1996). Entwicklung und Untersuchungen von Rodewerkzeugen für Zuckerrübenerntemaschinen. *Technische Universität Dresden. Fakultät Maschinenwesen. Dissertation A*.

Herrmann, K. (1996). Untersuchngen an höherfrequent schwingenden Polderscharen zur Zuckerrübenernte. *Technische Universität Dresden. Fakultät Maschinenwesen. Dissertation A*.

Kołodziej, P., Boryga, M. (2014). Frequency analysis of coupling with adjustable torsional flexibility. *Eksploatacja i Niezawodność – Maintenance and Reliability, 16*(2), 325-329.

Kołodziej, P., Stępniewski, A. (2007). Sprzęgło podatne. *Patent PL* 193910 B1.

Kołodziej, P., Gołacki, K. (2006). Stanowiska do badań sił reakcji korzeni buraka cukrowego na zadane typy obciążeń dynamicznych. *Inżynieria Rolnicza, 5*, 273-281.

Kołodziej, P., Boryga, M. (2017). Static analysis of the stresses of clutch components with infinitely variable adjustment of the torsional flexibility using FEM. *Mechanik, 11*, 1052-1054.

Korzybski, W., Rode, H. (2014). Systemy komputerowe w mechanice. *Logistyka, 6*, 5716-5724.

Łukaszewicz, K. (2017). Use of CAD software in the process of virtual prototyping of machinery. *7th International Conference on Engineering, Project, and Production Management, Procedia Engineering*, *182*, 425-433.

Malon, H., Garcia-Ramos, F.J., Vidal, M., Bone, A. (2016). Design and optimization of a chassis for an air-assisted sprayer with two fans using the finite element method. *Project Management and Engineering Research, 2014*. *Lecture Notes in Management and Industrial Engineering*, 103-115.

Pater, Z., Tomczak, J., Kołodziej, P., Boryga, M., Gołacki, K. (2017). Sprzęgło podatne. *Patent PL* 225230 B1.

Patyk, R., Kukiełka, L. (2009). Prognozowanie wytrzymałości zmęczeniowej zęba kultywatora z wykorzystaniem metod numerycznych. *Inżynieria Rolnicza, 9*(118), 181-187.

Pawłowski, T., Szczepaniak, J. (2005). Współczesna metodyka projektowania i weryfikacji konstrukcji maszyn rolniczych. *Inżynieria Rolnicza, 14*, 267-275.

Švrcek, M. (1995). Theoretische und experimentelle Untersuchungen an einem federnden Bodenlockerungswerkzeug im Hinblick auf mögliche Energieeinsparungen. *Technische Universität Dresden. Fakultät Maschinenwesen. Dissertation*.

ANALIZA NAPRĘŻEŃ WYORYWACZA BURAKÓW CUKROWYCH Z WYKORZYSTANIEM METODY ELEMENTÓW SKOŃCZONYCH

Streszczenie. W artykule przedstawiono sposób tworzenia modelu 3D, etapy przygotowania oraz wyniki analizy naprężeń wyorywacza kombajnu do buraków cukrowych z lemieszami płytowymi (polderowymi). W komputerowej symulacji uwzględniono przebiegi w czasie sił otrzymane z testów polowych. Do analizy wykorzystano moduł Analiza naprężeń programu Autodesk Inventor wykorzystujący metodę elementów skończonych. Wyniki analizy potwierdzają poprawność konstrukcji wyorywacza pod względem wytrzymałościowym. Największe naprężenia zredukowane obliczone wg hipotezy wynosiły 128,4 MPa (minimalna wartość współczynnika bezpieczeństwa odniesionego do granicy plastyczności wynosi 1,61). Dodatkowo omówiono budowę dwóch sprzęgieł podatnych mających możliwość bezstopniowej regulacji sztywności skrętnej, które mogą stanowić alternatywne rozwiązanie dla typowego układu podatnego w postaci amortyzatora oraz sprężyny śrubowej.

Słowa kluczowe: pasywny wyorywacz buraków cukrowych, analiza naprężeń, metoda elementów skończonych, układ z regulowaną sztywnością skrętną